



PERGAMON

Solid State Communications 113 (2000) 451–454

solid  
state  
communications

www.elsevier.com/locate/ssc

# Possibility of dynamic transitions in sliding charge-density waves

K.-i. Matsuda\*, S. Tanda

Department of Applied Physics, Hokkaido University, N13W8 Kita-ku, Sapporo 060-8628, Japan

Received 9 August 1999; received in revised form 27 October 1999; accepted 28 October 1999 by H. Akai

## Abstract

The transport properties of charge-density waves have been studied in orthorhombic TaS<sub>3</sub> as a function of the electric field. In the sliding state, we found that the power of the fundamental component of narrow-band noise has a minimum value at a bias voltage  $V_c$ . Moreover, the field dependence of the non-linear current carried by CDW changes abruptly at  $V_c$ . These results suggest the existence of a dynamic phase transition between *plastic-flow phase* and *fluid-solid phase*. © 2000 Elsevier Science Ltd. All rights reserved.

**Keywords:** A. Disordered systems; D. Noise

## 1. Introduction

The influence of randomly quenched impurities on the dynamics of driven interacting systems has been the subject of intense study. One area of particular interest has been the dynamics of disordered periodic systems, such as vortex lattices in the type II superconductors [1], Wigner crystals [2], Josephson junction arrays [3] and charge-density waves (CDWs) [4–7].

In the last case, below the CDW transition temperature  $T_{CDW}$ , electronic density is spatially modulated along the chain direction. In the absence of pinning due to impurities and lattice defects, CDWs have spatial long-range order and are free to slide. However, it has been argued that impurities destroy the spatial long-range order and pin the system. The dynamic properties of this system with quenched impurities have a close relation to crystal growth phenomena [8] described by the Kardar–Parisi–Zhang (KPZ) equation [9] and lead to very rich physics.

In recent theoretical studies [10,11], the existence of three dynamical phases has been predicted as a function of external driving force  $V$  provided by an electric field. The first regime is a *pinned phase*. For small  $V$ , the impurities pin CDWs and destroy their spatial long-range order. When the driving force exceeds a threshold driving force  $V_T$ , CDWs can de-pin and become mobile. The second regime ( $V_T < V$ ) is a *plastic-flow phase*. In this regime, the motion of

CDWs is highly non-uniform. For  $V$  far higher than  $V_T$  ( $V_T \ll V$ ), a dynamical phase transition occurs and CDWs moves into the third regime: *fluid–solid phase*. In this regime, despite the absence of true spatial long-range order and periodicity, CDWs have long-range *temporal* correlation.

The de-pinning transition between the pinned phase and the plastic-flow phase has already been studied and is fairly well understood [12,13]. In contrast, the dynamic phase transition between the plastic-flow phase and the fluid-solid phase has only recently begun to receive some attention and the existence of this transition has not yet been examined in CDWs experimentally.

In this paper, we report the experimental evidence of the existence of a dynamic phase transition in sliding CDWs. In the sliding states, the power of the fundamental component of the narrow-band noise (NBN) depends strongly on the bias voltage  $V$  and shows a minimum at a certain voltage  $V_c$ . The field dependence of the CDW current also changes at the same voltage  $V_c$ . The results indicate the existence of three phases in CDWs as a function of external driving force: the pinned phase ( $V < V_T$ ), the plastic-flow phase ( $V_T < V < V_c$ ), and the fluid-solid phase ( $V_c < V$ ).

## 2. Experimental

The orthorhombic TaS<sub>3</sub> (*o*-TaS<sub>3</sub>) crystals analyzed in this study were prepared using the chemical vapor method.

\*Corresponding author.

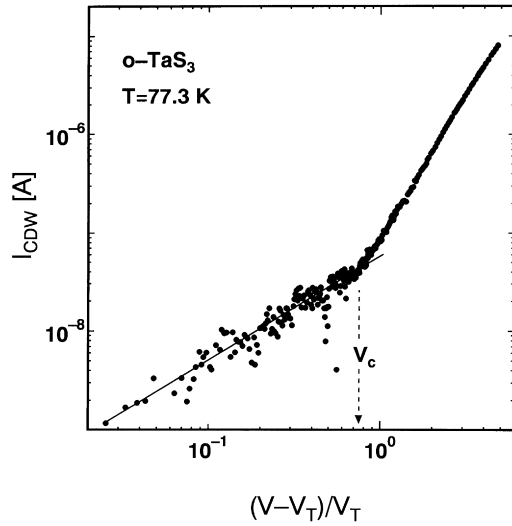


Fig. 1. Scaling plot of  $I_{\text{CDW}}$  obtained from the  $I$ - $V$  curves in  $o$ - $\text{TaS}_3$  at 77.3 K. The crossover exponent obtained from the solid-line is  $\zeta = 1.1 \pm 0.1$ .  $V_T = 34.5$  mV for this sample.  $I_{\text{CDW}}$  increases rapidly above  $V_c \approx 64.5$  mV.

Powder X-ray diffraction showed an orthorhombic phase for these crystals. We analyzed samples from the same preparation batch. Typical crystal dimensions were  $1 \text{ mm} \times 10 \mu\text{m} \times 1 \mu\text{m}$ , of which the longest dimension corresponds to the chain axis. The sample was placed on a glass substrate and electrical contacts were produced by evaporating gold in a vacuum. The length of each inter-contact arm was approximately 0.5 mm. The CDW transition temperature  $T_{\text{CDW}}$  is 214 K. The linear sample resistance was typically 1 k $\Omega$  at 77.3 K. We measured current-voltage characteristics and NBN in several samples. The current-voltage characteristics were measured using a four-probe configuration and a DC voltage-control technique. We assume that  $I$ - $V$  characteristics are described in terms of two-fluid model. In that case, the total current  $I$  can be written as  $I = I_n + I_{\text{CDW}}$ , where  $I_n$  is an ohmic component. Thus, the CDW current is calculated as  $I_{\text{CDW}} = (I - V)/R_n$ , where  $R_n$  is the resistance observed below the threshold voltage  $V_T$ .

The NBN measurements were carried out under fixed current condition. The main difficulty in performing these measurements was recording the small NBN signal of the sample. To solve this problem, we used a specially designed cryostat and an ultra-low-noise amplifier with a gain of 1000. A short cable was used between the sample and the amplifier to eliminate reflections and the effects of standing-waves. The signal was fed to a digital spectrum analyzer and each spectrum was obtained by averaging 8192 sweeps.

### 3. Result and discussion

Fig. 1 shows the bias dependence of the CDW current

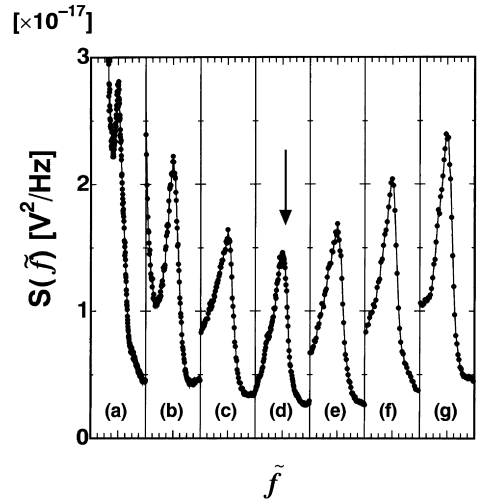


Fig. 2. The bias dependence of the spectrum of NBN in  $o$ - $\text{TaS}_3$  at  $T = 77.3$  K. The vertical axis represents the power of NBN in the unit of  $\text{V}^2/\text{Hz}$ . Each section shows the shape of fundamental NBN at each bias voltage. The width of fundamental NBN is normalized by the half-power band width  $\Delta f$  and the horizontal axis represents  $\tilde{f}$ , defined as  $\tilde{f} = (f - f_{\text{NBN}})/\Delta f$ . The parameters for each window are (a)  $V = 52.52$  mV,  $f_{\text{NBN}} = 405$  Hz,  $\Delta f = 97.55$  Hz; (b) 55.9 mV, 875 Hz, 96.30 Hz; (c) 60.45 mV, 2150 Hz, 133.75 Hz; (d) 65.98 mV, 4700 Hz, 340.60 Hz; (e) 73.26 mV, 10625 Hz, 469.40 Hz; (f) 83.97 mV, 24125 Hz, 685.70 Hz; and (g) 94.07 mV, 40375 Hz, 733.75 Hz, respectively.

$I_{\text{CDW}}$  above the threshold voltage  $V_T$ . The horizontal axis represents the reduced bias voltage  $(V - V_T)/V_T$ . For this sample,  $V_T$  is 34.5 mV. The solid line indicates the following power law form  $I_{\text{CDW}} \sim (V - V_T)^{1.1 \pm 0.1}$ . This result seems to be consistent with the theoretical prediction of depinning transition [12,13]. But recent theoretical [14] and experimental [15,16] work have shown that experimental systems are sufficiently small so that finite size effects make the critical regime unobservable. Thus the scaling behavior observed near  $V_T$  probably indicates crossover regime.

While the bias dependence of the CDW current near  $V_T$  obeys a scaling law, the  $I_{\text{CDW}}$ - $V$  curve bends at a field marked  $V_c$  and  $I_{\text{CDW}}$  increases abruptly for bias voltages above  $V_c$ . For this sample,  $V_c \sim 64.5$  mV. This remarkable increase of  $I_{\text{CDW}}$  implies that there is a different type of sliding state above  $V_c$ .

It is generally accepted that normal carriers play an important role in the dynamics of collective mode [26]. The uncondensate electrons screen the extra charge resulting from the CDW deformation, which is suppressed if they are absent. In fact, unusual  $I$ - $V$  characteristics have already been observed in some CDW materials ( $\text{NbSe}_3$  [17],  $\text{K}_{0.3}\text{MoO}_3$  [18]) at low temperature. They are discussed in relation with the vanishing screening effects in that temperature range. However, the bend in Fig. 1 is not caused by

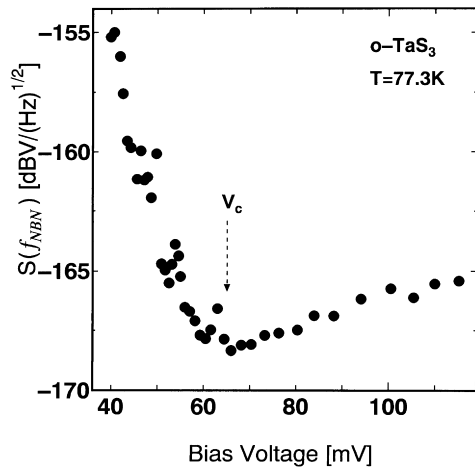


Fig. 3. The bias dependence of  $S(f_{\text{NBN}})$  at  $T = 77.3$  K. The vertical axis represents  $S(f_{\text{NBN}})$  in the unit of  $\text{dB V}/\sqrt{\text{Hz}} \equiv 10\log(\text{V}^2/\text{Hz})$ .  $S(f_{\text{NBN}})$  increases slowly above  $V_c$ .  $S(f_{\text{NBN}})$  is a minimum at  $V_c = 64.5$  mV for this sample, and increases with decreasing bias voltage below  $V_c$ .

screening effect since the motion of CDWs in the vicinity of  $V_c$  is much slower than the relaxation time of screening effect due to uncondensed electrons.

To get other information about the dynamics of CDWs, we measured the voltage fluctuation generated by sliding CDWs. In particular, the NBN reveals spatio-temporal order in CDWs. Thus, we investigated the power,  $S(f_{\text{NBN}})$ , and the fundamental frequency of NBN,  $f_{\text{NBN}}$ , as a function of the applied bias voltage. Fig. 2 shows the shapes of the fundamental component of the NBN for various values of

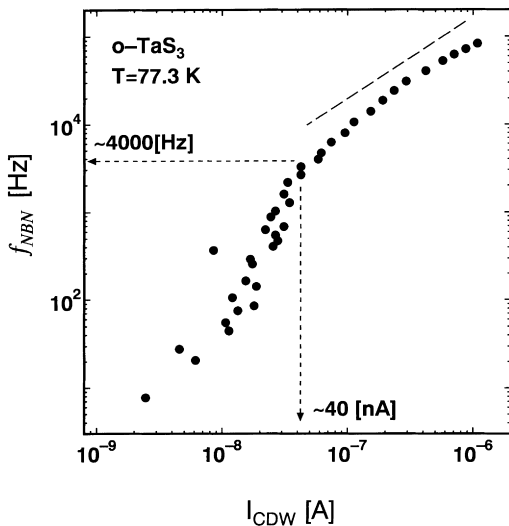


Fig. 4. The relationship between  $f_{\text{NBN}}$  and  $I_{\text{CDW}}$ . Above  $V_c$ ,  $I_{\text{CDW}}$  is proportional to  $f_{\text{NBN}}$ ; however, below  $V_c$ ,  $f_{\text{NBN}}$  is not proportional to  $I_{\text{CDW}}$ .

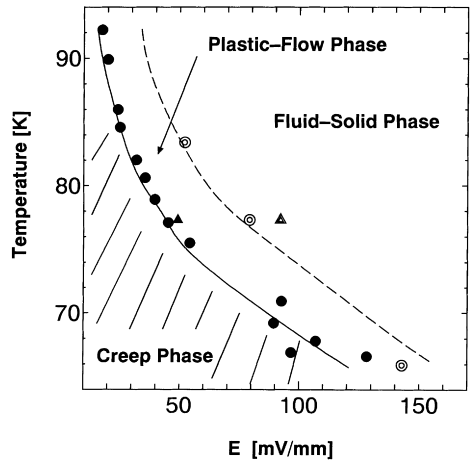


Fig. 5. Phase diagram in the DC-bias–temperature plane. The hatched region indicates the pinned state. Both solid and dashed lines are guides to the eyes for the experimental data.

applied electric voltage at 77.3 K. This measurement was actually performed under almost fixed current condition.

Thus,  $V$  represents the time-averaged DC value. The horizontal axis of each window represents a reduced frequency defined as  $\tilde{f} = (f - f_{\text{NBN}})/\Delta f$ , where  $\Delta f$  is a half-power bandwidth.

While both broad-band noise (BBN) and NBN were observed for voltages below  $V_c$  (2a–c), strong and sharp NBN was observed above  $V_c$  (2e–g). As the bias voltage increases,  $f_{\text{NBN}}$  moves into a higher frequency. However, the power of the NBN,  $S(f_{\text{NBN}})$ , decreases significantly in the range ( $V_T < V < V_c$ ) and shows a minimum in the vicinity of  $V_c$  (Fig. 2d).

The bias dependence of the power of the NBN is shown in Fig. 3. As the bias voltage increases in the range  $V_T < V < V_c$ , the power of NBN,  $S(f_{\text{NBN}})$ , decreases significantly. On the other hand, above  $V_c$ ,  $S(f_{\text{NBN}})$  increases slowly with the bias voltage. The bias dependence of the NBN observed above  $V_c$  is similar to that of the conventional NBN in CDWs [19–22] and was qualitatively described by the classical model [23–25] which treats CDW as a classical deformable object and does not allow the plastic motion. The bias dependence of  $S(f_{\text{NBN}})$  below  $V_c$  is not reported in previous experimental works. These results indicate that there are two regions in the sliding state as function of applied bias voltage.

In a recent theoretical study [10], the existence of a dynamical phase transition between the plastic-flow phase and the fluid-solid phase has been predicted. According to the theoretical prediction, below critical bias voltage  $V^*$ , the motion of CDWs is highly non-homogeneous. CDWs recover spatio-temporal order above  $V^*$ . The evidence of such a phase transition is a scaling behavior of  $S(f_{\text{NBN}} \sim |V - V^*|^\phi$  near  $V^*$ , where  $\phi$  is a dynamical critical exponent. As shown in Fig. 3, The power of the NBN,  $S(f_{\text{NBN}})$ ,

shows a minimum in the vicinity of  $V_c$ . This result supports the theoretical prediction.

If there are two different flow phases in the sliding state, another experimental evidence is expected in the relationship between  $I_{CDW}$  and  $f_{NBN}$ . Fig. 4 shows the relationship between the fundamental frequency of the NBN,  $f_{NBN}$  and the CDW current  $I_{CDW}$  at 77.3 K. The dashed line shown in Fig. 4 represents a linear relationship. The bias voltage  $V_c$  marked in both Figs. 1 and 3 approximately corresponds to  $f_{NBN} \approx 5$  kHz. Above  $f_{NBN} \geq 5$  kHz,  $I_{CDW}$  is approximately proportional to  $f_{NBN}$ . However, below  $f_{NBN} \leq 5$  kHz,  $I_{CDW}$  is not proportional to  $f_{NBN}$ . This result indicates that the number of electrons carried by CDW changes as a function of bias voltage below  $\sim 5$  kHz.

In the temperature range  $60 < T < 100$  K, well-defined  $V_T$  and  $V_c$  are observed. Fig. 5 shows the phase diagram in the DC-bias–temperature plane. The hatched region indicates the pinned state. We have used a solid line as a boundary between the pinned state and the plastic-flow phase, and dashed line as a boundary between the plastic-flow phase and the fluid-solid phase. Both  $V_T$  and  $V_c$  decrease with increasing temperature.

#### 4. Summary

The transport properties of charge-density waves (CDWs) in orthorhombic  $TaS_3$  (*o*- $TaS_3$ ) have been studied as a function of the electric field at 77.3 K. In the sliding state, we found that the power of the fundamental component of the NBN shows a minimum at a bias voltage  $V_c$ . Moreover, the field dependence of the non-linear current carried by CDW ( $I_{CDW}$ ) changes abruptly at  $V_c$ . Although it is difficult to evaluate the critical exponent  $\phi$  from the present available data, these results indicate the existence of a dynamical phase transition between the plastic-flow phase and the fluid-solid phase.

#### Acknowledgements

We would like to thank Prof K. Yamaya, Dr N. Hatakenaka, Prof Y. Okajima and Prof T. Sambongi for

their useful discussion. This study was supported in part by a grant from the Japan Society for the Promotion of Science for Young Scientists.

#### References

- [1] D.S. Fisher, M.P.A. Fisher, D.A. Huse, Phys. Rev. B 43 (1991) 130.
- [2] E.Y. Andrei, G. Deville, D.C. Glattli, F.I.B. Williams, E. Paris, B. Etienne, Phys. Rev. Lett. 60 (1988) 2765.
- [3] D. Dominguez, Phys. Rev. Lett. 72 (1994) 3096.
- [4] G. Grüner, Rev. Mod. Phys. 60 (1988) 1129.
- [5] L.P. Gor'kov, G. Grüner, Charge Density Waves in Solids, North-Holland, Amsterdam, 1989.
- [6] P. Monceau, Electronic Properties of Quasi-One-Dimensional Materials, Reidel, Dordrecht, 1985.
- [7] C. Schlenker, J. Dumas, M. Greenblatt, S. van Smaalen (Eds.), Physics and Chemistry of Low-Dimensional Inorganic Conductors Plenum, New York, 1996.
- [8] J. Krug, Phys. Rev. Lett. 75 (1995) 1795.
- [9] M. Kardar, G. Parisi, Y.C. Zhang, Phys. Rev. Lett. 56 (1986) 889.
- [10] L. Balents, M.P.A. Fisher, Phys. Rev. Lett. 75 (1995) 4270.
- [11] Lee-Wen Chen, L. Balents, M.P.A. Fisher, M.C. Marchetti, Phys. Rev. B 54 (1996) 12798.
- [12] D.S. Fisher, Phys. Rev. Lett. 50 (1983) 1486.
- [13] A.A. Middleton, D.S. Fisher, Phys. Rev. B 47 (1993) 3530.
- [14] C.R. Myers, J.P. Sethna, Phys. Rev. B 47 (1993) 11194.
- [15] J. McCarten, M. Maher, T.L. Adelman, R.E. Thorne, Phys. Rev. Lett. 63 (1989) 2841.
- [16] E. Sweetland, C.-Y. Tsai, B.A. Wintner, J.D. Brock, R.E. Thorne, Phys. Rev. Lett. 65 (1990) 3165.
- [17] G. Mihály, T. Chen, T.W. Kim, G. Grüner, Phys. Rev. B 38 (1988) 3602.
- [18] A. Maeda, M. Notori, K. Uchikura, Phys. Rev. B 42 (1990) 3290.
- [19] R.M. Fleming, C.C. Grimes, Phys. Rev. Lett. 42 (1979) 1423.
- [20] A. Zettle, G. Grüner, Phys. Rev. B 28 (1983) 2091.
- [21] F.Ya Nad', P. Monceau, Phys. Rev. B 46 (1992) 7413.
- [22] G. Mozurkewich, G. Grüner, Phys. Rev. Lett. 51 (1983) 2206.
- [23] H. Fukuyama, P.A. Lee, Phys. Rev. B 17 (1978) 535.
- [24] P.A. Lee, T.M. Rice, Phys. Rev. B 19 (1979) 3949.
- [25] H. Matsukawa, J. Phys. Soc. Jpn. 57 (1988) 3463.
- [26] P.B. Littlewood, Phys. Rev. B 36 (1987) 3108.